



## Article

# Characterization and Transcriptome Analysis Reveal Exogenous GA<sub>3</sub> Inhibited Rosette Branching via Altering Auxin Approach in Flowering Chinese Cabbage

Xinghua Qi <sup>1,†</sup>, Ying Zhao <sup>2,†</sup>, Ningning Cai <sup>2</sup>, Jian Guan <sup>1</sup>, Zeji Liu <sup>1</sup>, Zhiyong Liu <sup>1</sup>, Hui Feng <sup>1</sup> and Yun Zhang <sup>1,\*</sup>

<sup>1</sup> Department of Horticulture, Shenyang Agricultural University, 120 Dongling Road, Shenhe District, Shenyang 110866, China; qixinghua4858@163.com (X.Q.); philg1212@163.com (J.G.); liuzeji1315@163.com (Z.L.); liuzhiyong99@syau.edu.cn (Z.L.); fenghuiaaa@syau.edu.cn (H.F.)

<sup>2</sup> School of Functional Food and Wine, Shenyang Pharmaceutical University, Shenyang 110016, China; zhaoying941013@163.com (Y.Z.); c2827377601@163.com (N.C.)

\* Correspondence: zhangyun511@syau.edu.cn; Tel.: +86-024-88487143

† These authors contributed equally to this work.

**Abstract:** Branching is an important agronomic trait that is conducive to plant architecture and yield in flowering Chinese cabbage. Plant branching is regulated by a complex network mediated by hormones; gibberellin (GA) is one of the important hormones which is involved in the formation of shoot branching. Research on the regulatory mechanism of GA influencing rosette branch numbers is limited for flowering Chinese cabbage. In this study, the exogenous application of 600 mg/L GA<sub>3</sub> effectively inhibited rosette branching and promoted internode elongation in flowering Chinese cabbage. RNA-Seq analysis further found that these DEGs were significantly enriched in ‘the plant hormone signal transduction’ pathways, and auxin-related genes were significantly differentially expressed between MB and MB\_GA. The upregulation of auxin (AUX) and the upregulation of auxin/indole-3-acetic acid (AUX/IAA), as well as the downregulation of SMALL AUXIN-UPREGULATED RNA (SAUR), were found in the negative regulation of the rosette branching. The qRT-PCR results showed that the expression of AUX/IAA and SAUR from IAA gene family members were consistent with the results of transcriptome data. Phytohormone profiling by targeted metabolism revealed that endogenous auxin contents were significantly increased in MB\_GA. Transcriptome and metabolome analysis clarified the main plant hormones and genes underlying the rosette branching in flowering Chinese cabbage, confirming that auxin could inhibit rosette branching. In this regard, the results present a novel angle for revealing the mechanism of gibberellin acting on the branching architecture in flowering Chinese cabbage.

**Keywords:** flowering Chinese cabbage; branching; gibberellin; auxin; transcriptome



**Citation:** Qi, X.; Zhao, Y.; Cai, N.; Guan, J.; Liu, Z.; Liu, Z.; Feng, H.; Zhang, Y. Characterization and Transcriptome Analysis Reveal Exogenous GA<sub>3</sub> Inhibited Rosette Branching via Altering Auxin Approach in Flowering Chinese Cabbage. *Agronomy* **2024**, *14*, 762. <https://doi.org/10.3390/agronomy14040762>

Academic Editor: Caterina Morcia

Received: 4 March 2024

Revised: 29 March 2024

Accepted: 5 April 2024

Published: 8 April 2024



**Copyright:** © 2024 by the authors. Licensee MDPI, Basel, Switzerland. This article is an open access article distributed under the terms and conditions of the Creative Commons Attribution (CC BY) license (<https://creativecommons.org/licenses/by/4.0/>).

## 1. Introduction

Flowering Chinese cabbage (*Brassica campestris* L. ssp. *chinensis* [L.] Makino var. *utilis* Tsen et Lee) is an important and popular vegetable because of its high nutrient content and good flavor [1]. The major edible part of flowering Chinese cabbage is the stalk, the development of which has a direct impact on plant yield. The main species in Guangdong has one remarkable stalk per plant that can be harvested only once in production. A local variety, ‘Zengcheng flowering Chinese cabbage’, found in the Zengcheng District of Guangdong Province (23°26' N, 113°8' E), can be harvested multiple times because of the strong development of axillary branches on the rosette shoot.

The shoot branching of flowering Chinese cabbage is a vital characteristic that is conducive to improving crop yield and adaptability [2]. The branching system includes the main branch developed from the apical meristem, the lateral branch developed from the axillary meristem, and the primary rosette branch that grows from the basal rosette

leaves [3]. The bud can immediately grow, hibernate, or remain dormant after the formation of axillary buds. The activity of axillary buds is closely related to different endogenous and environmental stimuli, like plant hormones, nutrients, and light. The hormones involved in the network regulation of shoot branching include auxins, strigolactones (SLs), and cytokinins (CKs). However, further determination is needed on how these hormones interact to regulate the activation and growth of axillary buds in flowering Chinese cabbage.

Auxin is associated with axillary bud outgrowth and shoot branching formation by apical dominance [4]. The proliferation apex generates excess auxin, which is transported downwards to the stem to repress the growth of axillary buds and promote apical elongation. Removing the apex releases its inhibition on axillary buds, triggering the formation of branches. At present, some genes related to auxin transport that affect shoot branching formation have been reported. A mutant of *OsIAA6* in rice showed abnormal tiller outgrowth because of the regulation of the auxin transporter *OsPIN1* and tillering suppressor *OsTB1* [5]. In *Arabidopsis*, the major auxin influx carrier is AUXIN INFLUX CARRIER PROTEIN 1 (AUX1), whereas the main auxin efflux carrier is PIN-FORMED1 (PIN1) because it facilitates efficient auxin export from cells [6–9]. Exploring the genes involved in auxin transport is of great significance for revealing the shoot branching mechanism of flowering Chinese cabbage. Furthermore, other phytohormones also play important roles during the initiation of shoot branching. CKs promote shoot branching by upregulating the expression of *PIN3*, *PIN4*, and *PIN7* on the basal plasma membrane of xylem parenchyma cells [10]. The branching regulation of SL signaling pathways involves the MAX genes, which lead to the polyubiquitination and 26S-proteasome-mediated degradation of D53 by the receptor D14 and the recruitment of the SCF complex in *Arabidopsis* [11]. ABA inhibits the growth of lateral buds by the transcription factor BRANCHED1 (BRC1), which promotes ABA synthesis by activating the expression of the transcription factor family HOMEOBOX PROTEIN (HB), including NCED3 in *Arabidopsis* [12]. In addition, the SL and BR signaling pathways commonly regulate and control shoot branching via MAX2-induced degradation of *bri1*-EMS-suppressor 1 (BES1) [13].

Bioactive gibberellin (GA) is a diterpenoid plant hormone that undergoes biosynthesis through complex pathways and controls almost all plant development processes throughout the plant life cycle [14]. The bioactive GAs are GA<sub>1</sub>, GA<sub>3</sub>, GA<sub>4</sub>, and GA<sub>7</sub> in higher plants [15]. GAs is also a plant hormone that plays an important role in the regulation of bud outgrowth, the specific role of GAs in branching has been characterized well [16–18]. GAs are often considered to be branching inhibitors because the shoot branching phenotype has been observed in GA biosynthesis mutants of *Arabidopsis* and in genetically modified plants of different species lacking GAs. For example, gibberellin inhibits the formation of axillary buds in *Arabidopsis* by regulating the activity of the DELLA-SPL9 complex [19]. Transgenic rice overexpressing *GA2oxs*, which normally limits bioactive GA levels, exhibited early and increased tillering by inactivating endogenous and exogenous bioactive GAs [20]. In rice, high GA levels can stimulate APC/CTE to facilitate the degradation of *MOC1* in the AM, leading to restricted tillering [21]. In aspen plants, a decrease in the biological activity of GAs leads to significantly higher lateral buds compared to the wild type [22]. GAs negatively regulate the formation of axillary buds by overexpression of the GA metabolic gene *GA2ox*, leading to an increased number of tillers in turfgrass [23]. In a suppressor of runnerless strawberry mutant (*srl*), FveRGA1, encoding a DELLA protein, negatively regulates stolon formation [24]. Contrary to the above results, some studies have shown that GAs can promote shoot branching. In the perennial woody plant *Jatropha curcas*, GAs and CKs both negatively influence BRC1 and BRC2 expression to synergistically promote lateral bud outgrowth [25]. The growth of axillary buds in a GA biosynthesis mutant is restricted, while the application of bioactive GA rescues the phenotype in strawberries [26]. In sweet cherries, spraying GA<sub>3</sub> can promote the growth of lateral branches [27]. However, GA<sub>3</sub> under light-induced sugar metabolism contributes to bud burst, as been reported in rose [28]. Moreover, when exogenous spraying of GA<sub>3</sub>, GA<sub>4</sub>, and GR<sub>24</sub> was performed

on aspen trees, GA<sub>3</sub> induced shoot branching from axillary bud abscission whereas GA<sub>4</sub> promoted outgrowth [29].

Plant growth regulators have been widely used to improve crop yield and quality. In recent years, there has been increasing interest in the exogenous application of GA<sub>3</sub> to regulate plant growth and development. In a previous study, we constructed a gene mapping population in flowering Chinese cabbage using the non-branching double haploid line 'CX010' and the multiple branching double haploid line 'CX020' as parents, and the two tandem genes *BraA07g041560.3C* and *BraA07g041570.3C*, which encode gibberellin 2-oxidase that in turn acts on C19 gibberellins, were obtained by a map-based cloning strategy [30]. One of the two genes negatively regulated the formation of shoot branching in flowering Chinese cabbage. Hence, we chose to spray GA<sub>3</sub> to explore the potential molecular mechanism of gibberellin affecting flowering Chinese cabbage branching. In this study, comparative transcriptome analysis was used to characterize the gene expression profiles and high-performance liquid chromatography (HPLC) was used to test the levels of plant hormone content. We analyzed GA<sub>3</sub> to inhibit the branching of rosette shoots in flowering Chinese cabbage by affecting the auxin signaling pathway. Our study provides novel information for clarifying the molecular mechanism of flowering Chinese cabbage varieties.

## 2. Materials and Methods

### 2.1. Plant Materials and Exogenous GA<sub>3</sub> Spraying Treatment

CX020 (MB) is a multiple-branch phenotype isolated by microspore culture to obtain a double haploid (DH) line of Zengcheng flowering Chinese cabbage. This is a pure line in the genetic sense. The experimental materials were planted in the experimental field of Shenyang Agricultural University (41°79' N, 123°4' E). In spring 2019, the seeds were directly sowed into a 50-hole tray, and after 20 days, the pots were changed to a red plastic bowl with a diameter of 15 cm to conveniently observe the phenotypic changes. Exogenous GA<sub>3</sub> (Solarbio, Beijing, China) with different concentrations (200, 400, 600, 800, and 1000 mg/L) was applied to the whole plant (except for the roots) when the third euphylla had grown and was carried out once every two days for a total of 3 times. Each concentration consisted of 10 plants with 3 replicates. The control material was separately sprayed with distilled water. Finally, 600 mg/L was selected as the optimal spraying concentration. The branching traits appeared after 40 days of spraying GA<sub>3</sub>. To reduce differences between plants, 3 plants were selected from each of MB and MB\_GA, and basal parts of 3 cm were randomly collected from each group of plants. All of the stems collected from three MB or MB\_GA plants were mixed together to obtain a library, named MB\_1, MB\_2, MB\_3, MB\_GA\_1, MB\_GA\_2, and MB\_GA\_3. All samples were frozen in liquid nitrogen and then stored in a -80 °C freezer to sequence transcriptomes and to measure hormone content.

### 2.2. RNA Extraction and Transcriptome Sequencing

Total RNA was extracted using a Plant RNAPrep Pure Micro Kit (TIANGEN, Beijing, China). The concentration, quality, and integrity were determined using a NanoDrop spectrophotometer (Thermo Fisher Scientific, Waltham, MA, USA). Three micrograms of RNA were used as the input material for the RNA sample preparations. Sequencing libraries were generated using the TruSeq RNA Sample Preparation Kit (Illumina, San Diego, CA, USA), as per the manufacturer's instructions. In order to select cDNA fragments of the preferred 200 bp length, the library fragments were purified using the AMPure XP system (Beckman Coulter, Beverly, CA, USA) [31]. DNA fragments with ligated adaptor molecules on both ends were selectively enriched using the Illumina PCR Primer Cocktail in a 15 cycle PCR reaction. The products were purified (AMPure XP system) and quantified using an Agilent high-sensitivity DNA assay on a Bioanalyzer 2100 system (Agilent, Suzhou, China). The library was sequenced on a Hiseq platform (Illumina, San Diego, CA, USA).

### 2.3. Transcriptome Analysis

The clean reads were mapped to the brassica reference genome (<http://brassicadb.cn/#/> (accessed on 9 March 2020)). The combination of false discovery rate (FDR)  $\leq 0.001$  and the absolute value of log2Ratio  $\geq 1$  were used as the threshold for judging significant different gene expression levels [32–34]. In the study, genes with a threshold value of  $|\log_2 \text{ratio}| \geq 1.0$  and a false discovery rate (FDR)  $\leq 0.01$  were defined as possessing significant differential gene expression (DEGs). The trend analysis was performed by the genescloud tools (<https://www.genesccloud.cn>, accessed on 9 March 2020).

Gene set enrichment analysis for Gene Ontology (GO) was performed using the topGo 2.54.0 package (Sunovo Hulian, Beijing, China). ClusterProfiler was used to perform KEGG enrichment analysis. The gene list and gene number of each pathway were calculated using the differential genes annotated by the KEGG pathway. The hypergeometric distribution method was used to calculate  $p \leq 0.05$ , and compared with the background of the entire genome, to determine the differences between the main biological functions of the genes [35].

### 2.4. Metabolite Profiling of Hormone Content Using UPLC-MS/MS

Next, 3 cm stem parts were sampled with 3 biological replicates for each group of samples to measure hormone content. Fresh plant materials were harvested, weighed, immediately frozen in liquid nitrogen, and stored at  $-80^{\circ}\text{C}$  until needed. Plant materials (50 mg fresh weight) were frozen in liquid nitrogen, ground into powder, and extracted with 1 mL methanol/water/formic acid (15:4:1, *v/v/v*). The combined extracts were evaporated to dryness under a nitrogen gas stream, reconstituted in 100  $\mu\text{L}$  of 80% methanol (*v/v*), and filtered through a 0.22  $\mu\text{m}$  pore size, 14 mm diameter filter for further LC-MS analysis. The sample extracts were analyzed using an UPLC-ESI-MS/MS system. The LC column used was a Waters ACQUITY UPLC HSS T3 C18 (100 mm  $\times$  2.1 mm i.d. 1.8  $\mu\text{m}$ ). The HPLC effluent was connected to an electrospray ionization (ESI)-triple quadrupole-linear ion trap-MS/MS system (Applied Biosystems 4500 Q TRAP) [36]. A specific set of MRM transitions was monitored for each period, as determined by the plant hormones eluted within this period.

### 2.5. Real-Time Quantitative PCR Analysis (qRT-PCR)

Transcriptome gene expression was analyzed using real-time quantitative PCR (qRT-PCR). cDNA was prepared using an iScript<sup>TM</sup> cDNA Synthesis Kit according to the manufacturer's protocol. qRT-PCR was performed using a Bio-Rad CFX96 real-time system with SYBR<sup>®</sup> Green PCR Supermix (Hercules, CA, USA). Each system contained 10.4  $\mu\text{L}$  of SYBR mixture, forward and reverse primers, 8.8  $\mu\text{L}$  of  $\text{H}_2\text{O}$ , and 0.8  $\mu\text{L}$  of cDNA in a total final volume of 20  $\mu\text{L}$ . This technique was repeated three times. The following qRT-PCR program was used: 98  $^{\circ}\text{C}$  for 30 s, followed by 39 cycles of a two-step reaction (98  $^{\circ}\text{C}$  for 15 s and 60  $^{\circ}\text{C}$  for 30 s). The 2- $\Delta\Delta\text{CT}$  method was used to calculate the relative expression levels [37]. *Actin* gene was used as a control. To verify the expression levels detected by RNA-seq, the RNA-seq data were compared to the data obtained by qRT-PCR. DEGs were identified by two-fold change ( $\log_2 \text{ratio} \geq 2$ ). The primers are listed in Supplementary Materials. All reactions were performed with three technical and biological replicates, and three independent biological replicates were conducted for all the qRT-PCR reactions.

### 2.6. Statistical Analysis

The data were determined using the *t*-test with IBM SPSS Statistics 23 software (IBM, New York, NY, USA) at the 0.05 level to compare the significant differences. Maps were generated in Origin 2018 (OriginLab, Guangzhou, China).

### 3. Results

#### 3.1. Exogenous GA<sub>3</sub> Obviously Inhibited Rosette Branching

'CX020 (MB)' plants formed a multiple-branch phenotype, the cauline branching numbers increased from when sprayed with GA<sub>3</sub> (Figure 1A,B) and the rosette branching numbers decreased from when sprayed with GA<sub>3</sub> (Figure 1C,D) when the cauline and the rosette branching numbers were counted during harvest. The total number of cauline branches, 15.20, was significantly greater in the MB\_GA group than in the MB group. The number of rosette branches were 3.40 and 9.04 in the MB\_GA and MB groups, respectively, which was significantly lower in the MB\_GA group than in the MB group (Figure 2A). This result revealed that the effect of GA on the branching phenotype of MB was noticeably different. In addition, the length of the internode in the MB\_GA group was significantly different from that in the MB group (Figure 2B). These results showed that GAs influence rosette branching from the first to the fourth node and may limit the growth of lateral branches in flowering Chinese cabbage.

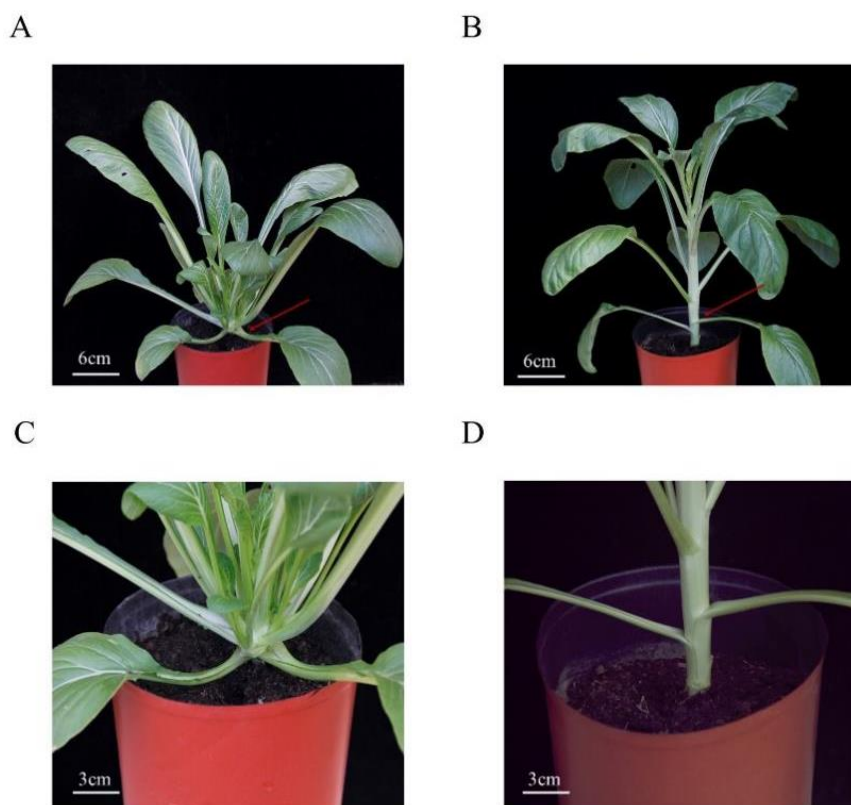


**Figure 1.** Phenotypes of MB and MB with 600 mg/L of GA<sub>3</sub> treatment. The entire plant appearance of MB (A) and MB after 600 mg/L of GA<sub>3</sub> treatment (B). The phenotype of rosette branching in MB (C) and MB after 600 mg/L of GA<sub>3</sub> treatment (D). The rosette branching is indicated with red arrows.

#### 3.2. Influences of Exogenous GA<sub>3</sub> on Gene Expressions

To determine the DEGs involved in the regulatory mechanisms of branching, we performed an integrated transcriptome analysis of MB and MB\_GA and sequenced six cDNA libraries (two samples with three replicates). A total of 379.9 million high-quality reads were generated, constituting 57.4 GB of cDNA sequences. The Q30 value (sequence error rate was 0.1%) of each sample was no less than 93.7%. To further define the quality of sequencing, 90.36% of read coverage was analyzed, representing the percentage of a gene covered by the reads (Tables S1 and S2). The GC content of the six libraries was 47.26%, 47.17%, 47.18%, 47.22%, 47.21%, and 47.21%, respectively. The comparison efficiency between the reads and the reference genome of each sample was between 94.4% and 95.26% (Tables S3 and S4). We first counted the scatter plot to confirm gene expression levels in the

samples and generated a heatmap plot to show changes in the six libraries (Figure 3A). The RNA-seq data from the biological replicates were found to co-cluster when assessed using principal component analysis (PCA). The results of the PCA plot were consistent across the biological replicates (Figure 3B). The volcano plot shows that there were more genes with multiple significant differences among the upregulated genes, while the difference multiple of downregulated genes was smaller (Figure 3C).

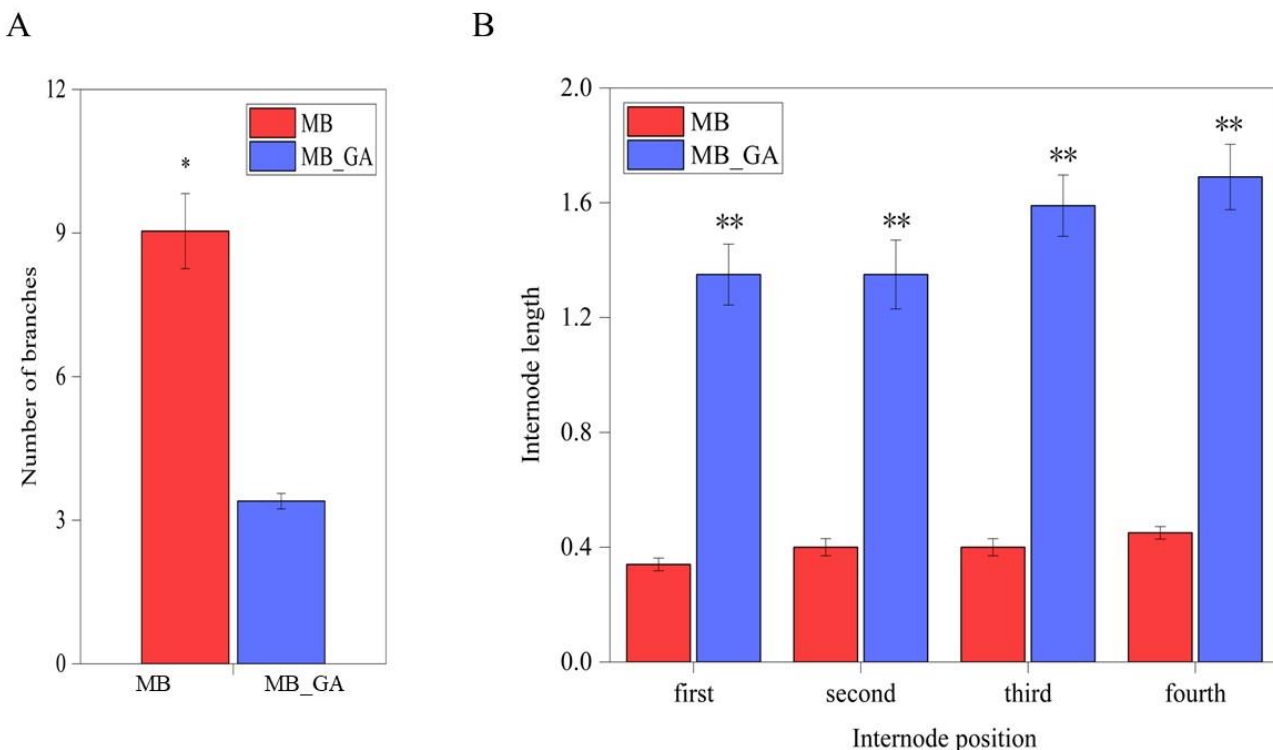


**Figure 2.** The primary rosette branch numbers of MB and MB\_GA (**A**). Relationship between internode position and internode length (**B**). \* and \*\* indicate significant differences in expression levels at  $p < 0.05$  and  $p < 0.01$  between the two types as determined according to the *t*-test.

To identify the genes involved in the formation and development of branching, significant DEGs (with the filter criteria set as fold change  $\geq 2.0$  and FDR  $\leq 0.001$ ) were obtained for the two types of plants (MB and MB\_GA) (Tables S5 and S6). As a result, 2183 DEGs were identified between MB and MB\_GA, of which 1318 were upregulated and 865 were downregulated in MB versus MB\_GA (Figure 3D). The number of downregulated DEGs was higher than that of the upregulated DEGs.

All 2183 DEGs were classified into eight trend clusters with an algorithm developed from gene expression trends ( $\text{RPKM} \geq 2$ , FDR  $\leq 0.001$  and  $|\log_2(\text{ratio})| \geq 1$ ). The results showed that in the clusters 1, 2, 3, and 4, the gene expression decreased obviously from MB to MB\_GA, containing 941 genes, and in the clusters 5, 6, 7, 8, and 9, the gene expression increased obviously from MB to MB\_GA, containing 1242 genes (Figure 4). These results indicate that the transcriptome data are reliable.

### 3.3. Enrichment Analysis for the DEGs

To further confirm the biological functions and assign genes related to branching, DEGs were mapped using GO terms to classify their functions ( $p \leq 0.05$ ), and the top 20 enriched pathways were used to make the GO enrichment map (Figure 5A). We identified 144 enriched GO terms that were assigned, including 73 under biological processes, 55 under molecular functions, and 16 under cellular components (Table S7). Under biological processes, the subcategories were related to biological regulation (GO: 0008152; 1043DEG) and regulation of metabolic processes (GO: 0019222; 236DEG), and the subcategories related

to hormones were response to hormones (GO: 0009725; 37DEG) and response to auxin (GO: 0009733; 32DEG). Under molecular function, the subcategories were related to catalytic activity (GO: 0003824; 986DEG) and DNA binding (GO: 0003677; 302DEG).

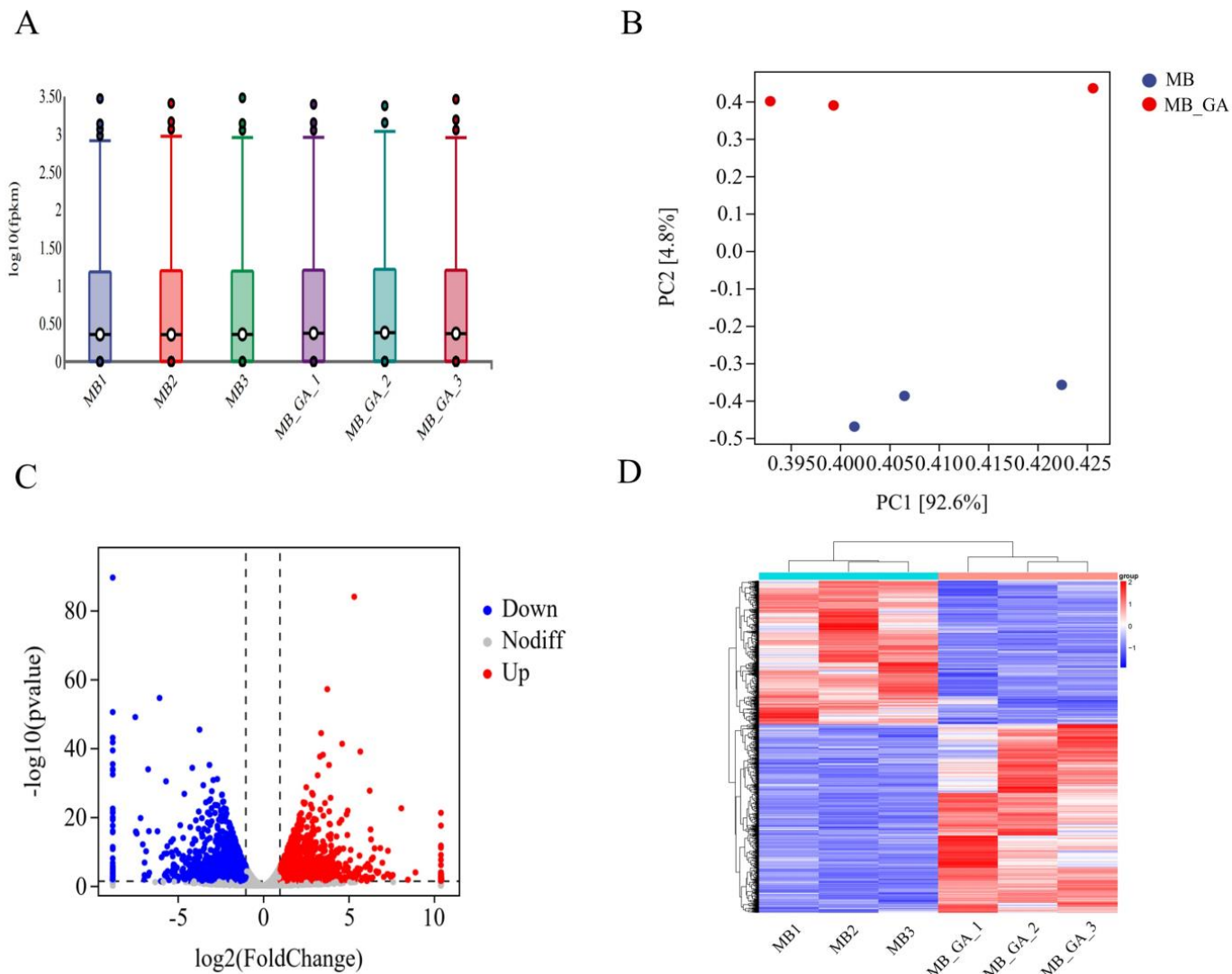


**Figure 3.** Comparative analysis of expression patterns of differentially expressed genes (DEGs) in six segments of MB. Hierarchical cluster diagram of gene expression level in samples. MB1, MB2, and MB3 are controls; MB\_GA\_1, MB\_GA\_2, and MB\_GA\_3 are the experimental groups treated with 600 mg/L GA<sub>3</sub> (A). Principal component analysis (PCA) of the differentially expressed genes between MB and MB\_GA (B). Volcano plot of the differentially expressed genes between MB and MB\_GA. Blue indicates downregulation of the gene, red indicates upregulation of the gene, and gray indicates non-regulation of the gene (C). The number of up- and down-regulated expressed genes (D).

To further identify genes associated with metabolic pathways, a total of 771 DEGs were mapped to 41 KEGG pathways (Table S8). The top 20 KEGG pathways were significantly enriched (Figure 5B, Table 1). The plant hormone signal transduction pathway (brp04075; 74) was the largest category, which was significantly enriched compared to other pathways, followed by phenylpropanoid biosynthesis (brp00940; 51) and starch and sucrose metabolism (brp00500; 39). These results indicate that hormone signal transduction was highly enriched in branching development, suggesting the complexity of the mechanisms underlying the development of branching in plants.

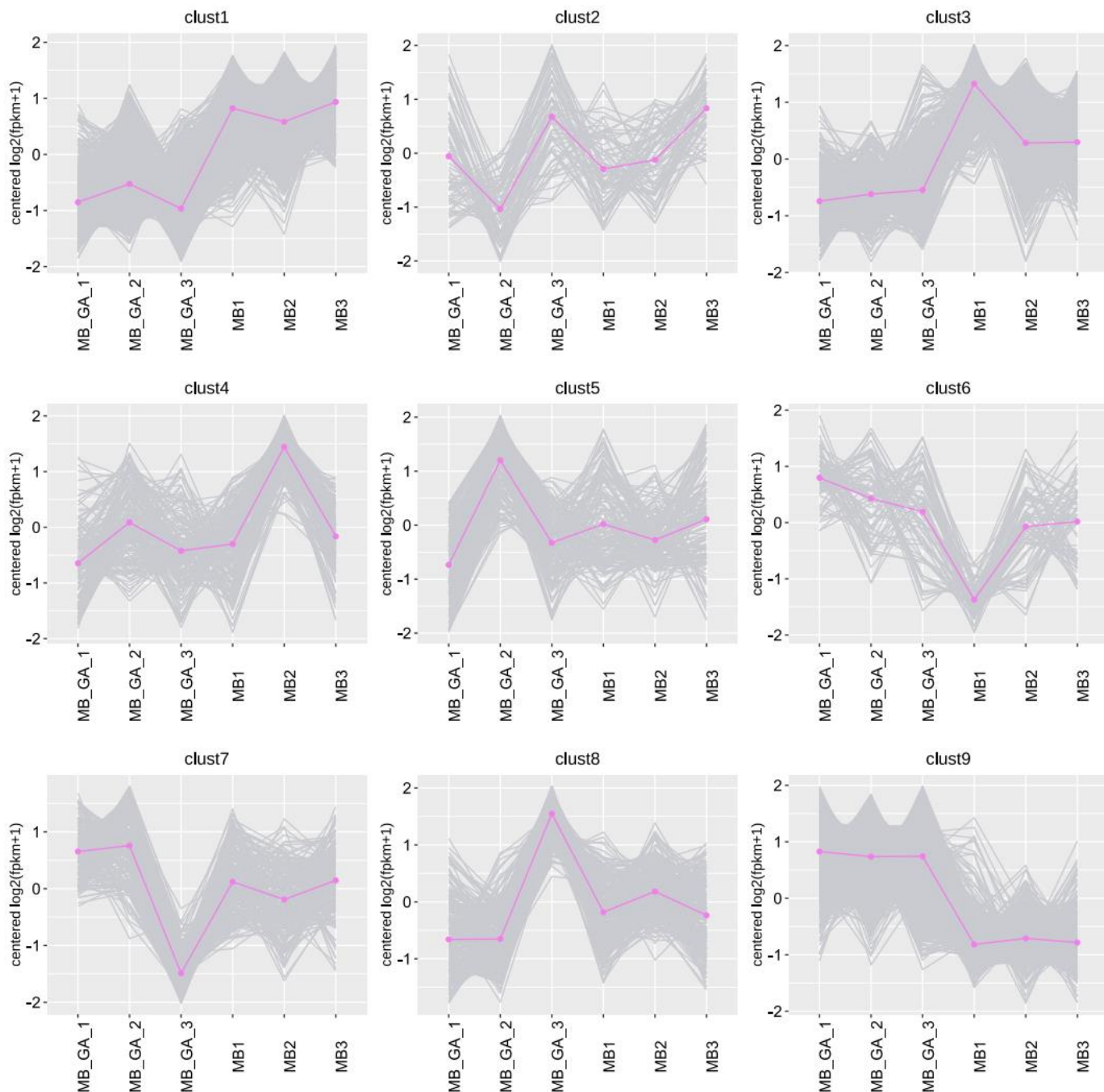


**Figure 4.** The trend analysis of the expression profile of all DEGs in all six pairwise comparisons. The *y*-axis represents the clustering groups of the gene expression level and the *x*-axis represents the different samples.

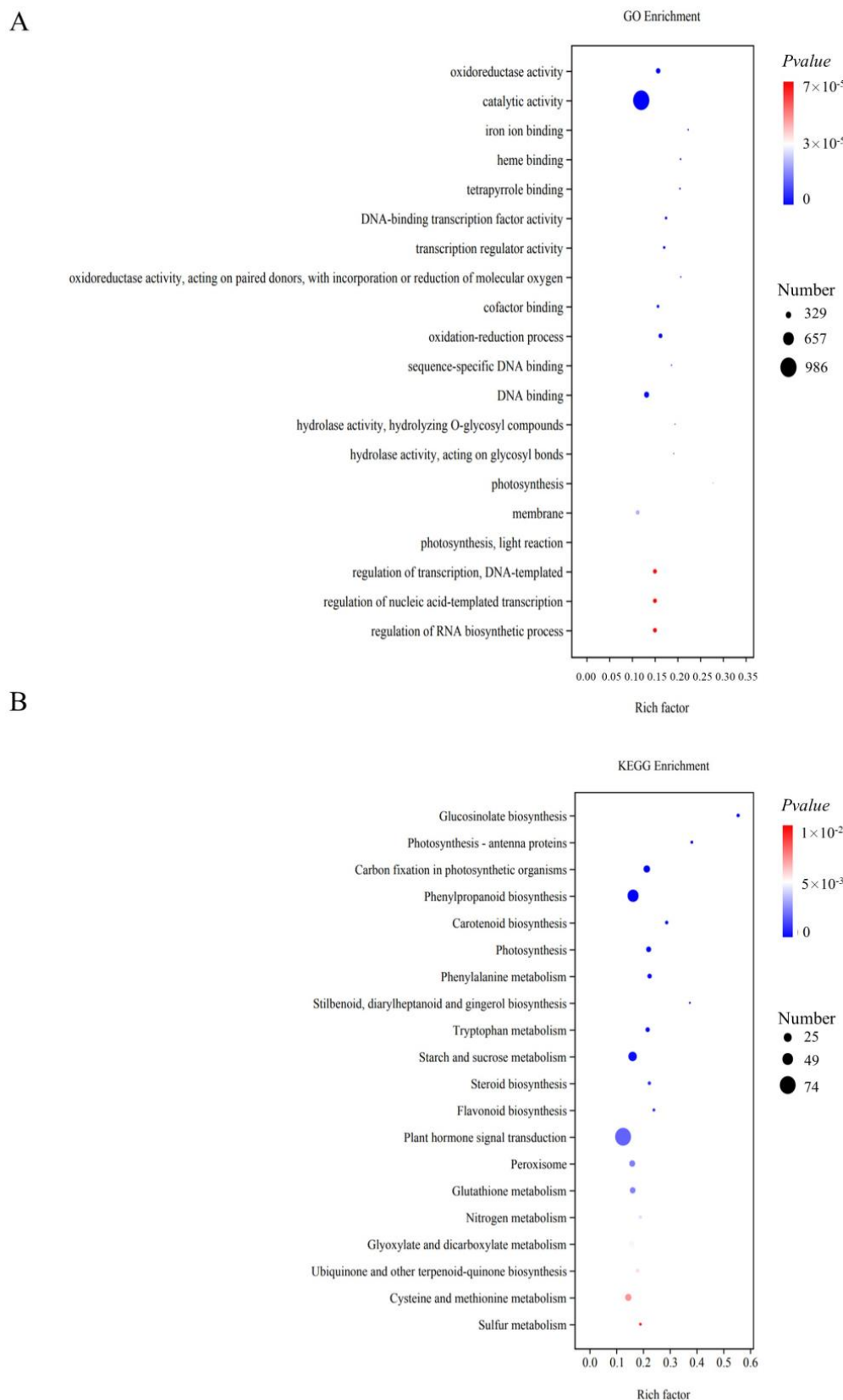


**Figure 5.** Twenty most significantly enriched GO and KEGG metabolic pathways. (A) GO enrichment analysis for MB vs. MB\_GA; (B) KEGG enrichment analysis for MB vs. MB\_GA.

**Table 1.** Significantly enriched KEGG pathways of DEGs in MB vs. MB\_GA.

Pathway ID	Pathway	DEG (%)	Total DEGs	Adjust p Value
brp04075	Plant hormone signal transduction	74 (9.60%)	771	$1.73 \times 10^{-2}$
brp00940	Phenylpropanoid biosynthesis	51 (6.61%)	771	$6.20 \times 10^{-4}$
brp00500	Starch and sucrose metabolism	39 (5.06%)	771	$2.91 \times 10^{-3}$
brp04626	Plant–pathogen interaction	38 (4.93%)	771	$3.54 \times 10^{-1}$
brp04016	MAPK signaling pathway—plant	32 (4.15%)	771	$6.81 \times 10^{-2}$
brp00710	Carbon fixation in photosynthetic organisms	30 (3.90%)	771	$2.24 \times 10^{-4}$
brp00270	Cysteine and methionine metabolism	29 (3.76%)	771	$4.43 \times 10^{-2}$
brp04146	Peroxisome	27 (3.50%)	771	$1.95 \times 10^{-2}$
brp00480	Glutathione metabolism	26 (3.37%)	771	$1.95 \times 10^{-2}$
brp00630	Glyoxylate and dicarboxylate metabolism	24 (3.11%)	771	$3.32 \times 10^{-2}$
brp00230	Purine metabolism	24 (3.11%)	771	$3.19 \times 10^{-1}$
brp00195	Photosynthesis	23 (2.98%)	771	$8.07 \times 10^{-4}$
brp00260	Glycine, serine, and threonine metabolism	21 (2.72%)	771	$5.77 \times 10^{-2}$
brp00040	Pentose and glucuronate interconversions	21 (2.72%)	771	$4.72 \times 10^{-1}$
brp00360	Phenylalanine metabolism	20 (2.60%)	771	$1.71 \times 10^{-3}$
brp00380	Tryptophan metabolism	20 (2.60%)	771	$2.16 \times 10^{-3}$
brp00130	Ubiquinone and other terpenoid–quinone biosynthesis	16 (2.08%)	771	$3.71 \times 10^{-2}$
brp00561	Glycerolipid metabolism	16 (2.08%)	771	$2.49 \times 10^{-1}$
brp00966	Glucosinolate biosynthesis	15 (1.95%)	771	$1.41 \times 10^{-7}$
brp00906	Carotenoid biosynthesis	15 (1.95%)	771	$8.07 \times 10^{-4}$

Total DEGs: total number of DEGs with pathway annotations. Percentage (%) =  $100\% \times (\text{number of DEGs})/\text{total number of DEGs}$ .

### 3.4. DEGs in Plant Hormones Related to Branching

In KEGG enrichment analysis, we observed that the plant hormone signaling pathway involved the most differentially expressed genes (Table S9). Based on this, we further studied plant hormone-related genes. Of these, 40 DEGs were enriched in the IAA signal transduction pathway, indicating a potential connection between auxin and GA. The DEGs of the primary auxin-response factors included auxin1 (*AUX1*), auxin/indole-3-acetic acid (*AUX/IAA*), SMALL AUXIN-UPREGULATED RNA (*SAUR*), and *GH3* involved in IAA biosynthesis [38]. Only one *AUX1* gene (*BraA04g027030.3C*) was annotated which showed log<sub>2</sub> ratios of 2.268 in MB\_GA/MB. *AUX/IAA* genes (*BraA01g031100.3C*, *BraA05g024120.3C*, *BraA03g054630.3C*, *BraA01g035920.3C*, *BraA01g008880.3C*, *BraA03g040660.3C*, *BraA03g057220.3C*, *BraA03g017680.3C*, *BraA03g040670.3C*, *BraA06g001750.3C*) were annotated of which 10 DEGs may be associated with plant branching. Twenty-four *SAUR* genes were annotated, of which eight genes (*BraA09g050440.3C*, *BraA05g001150.3C*, *BraA04g032240.3C*, *BraA05g009190.3C*, *BraA10g011930.3C*, *BraA01g013230.3C*, *BraA04g025770.3C*, *BraA03g023650.3C*) were upregulated in MB\_GA and sixteen genes (*BraA07g016220.3C*, *BraA01g006580.3C*, *BraA10g022020.3C*, *BraA02g007500.3C*, *BraA07g002710.3C*, *BraA07g039120.3C*, *BraA01g003540.3C*, *BraA10g022020.3C*, *BraA01g003530.3C*, *BraA01g003550.3C*, *BraA06g044670.3C*, *BraA01g000130.3C*, *BraA02g022940.3C*, *BraA02g007480.3C*, *BraA01g003510.3C*, *BraA08g015690.3C*) were downregulated in MB\_GA. Five *GH3* genes (*BraA03g053600.3C*, *BraA10g025440.3C*, *BraA02g013860.3C*, *BraA09g054360.3C*, *BraA06g004330.3C*) were upregulated in MB\_GA. The *GH3* upregulated genes showed log<sub>2</sub> ratios of 2.255, 1.260, 1.232, 1.873, and 1.823, respectively (Figure 6A).

Cytokinins are often used as the second messenger of auxins to regulate branching development [39]. Two *ARABIDOPSIS RESPONSE REGULATOR* (*B-ARR*) genes (*BraA07g012270.3C*, *BraA03g046670.3C*) were annotated. Ten genes had relevance to the ABA signal, including *BraA03g029760.3C*, *BraA03g002100.3C*, *BraA05g005770.3C*, *BraA10g000590.3C*, *BraA03g021430.3C*, *BraA07g024750.3C*, *BraA03g020010.3C*, *BraA06g027110.3C*, *BraA05g018520.3C*, and *BraA10g016990.3C* (Figure 6A).

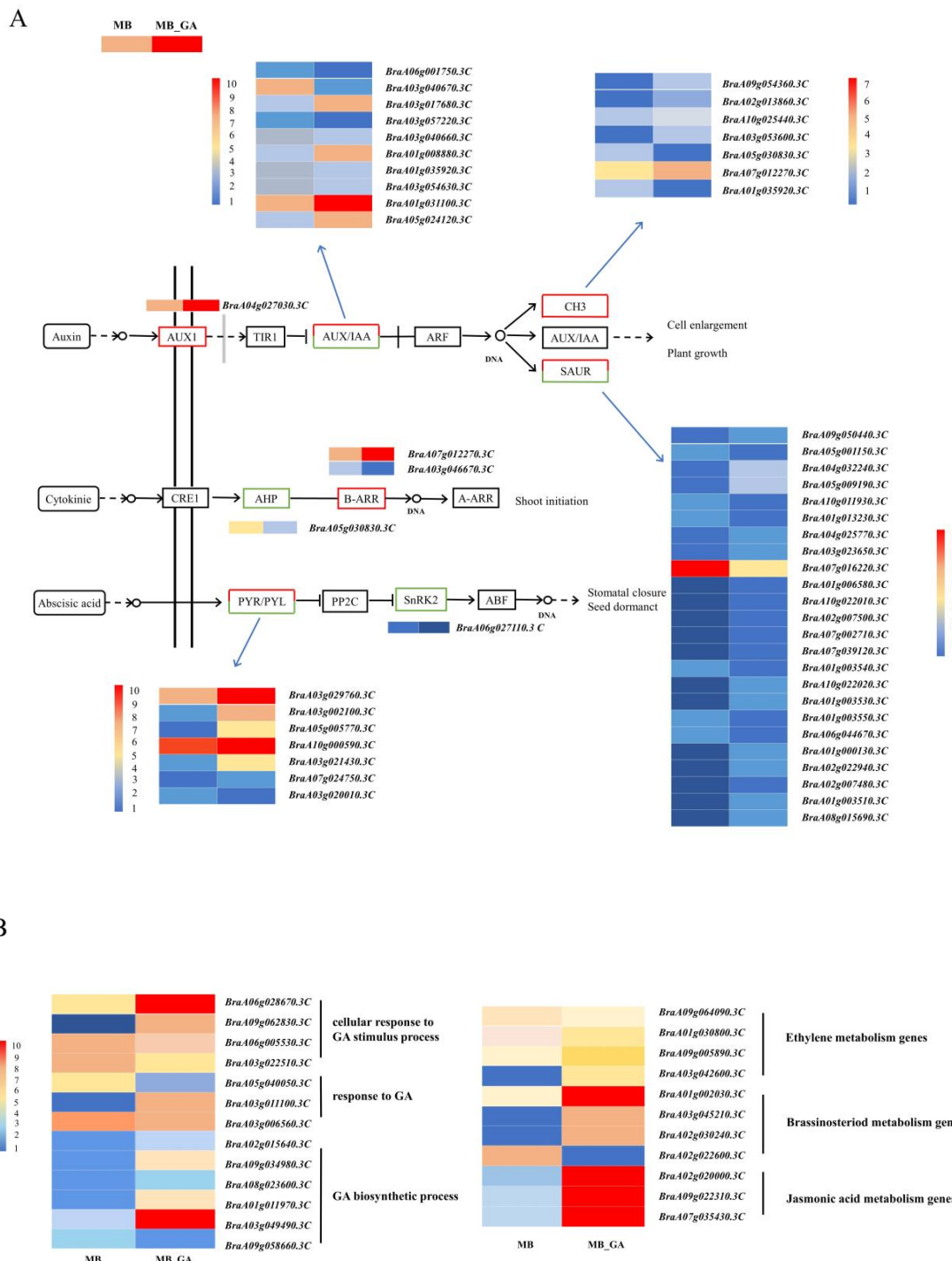


**Figure 6.** Expression of differentially expressed genes involved in the plant hormone genes (auxin, cytokinin, abscisic acid). Note: The bar on the right represents the relative expression values. Upregulated genes are marked with red borders and downregulated genes with green borders. Unchanged genes are marked with black borders (A). Expression of differentially expressed genes involved in the plant hormone genes (gibberellin, ethylene, brassinosteroid, jasmonic acid) (B).

Gibberellin has an important effect not only on internode elongation but also on branching development. In rice, auxin and gibberellin can regulate the negative gravity response of the stem by antagonizing the expression of *XYLOGLUCAN ENDOTRANSGLYCOSYLASE* (*XET*) [40,41]. We detected two *XET* genes (*BraA10g015660.3C*, *BraA02g012200.3C*) that were upregulated in the MB. In the GA signal transduction pathway, we detected one differ-

entially expressed GA INSENSITIVE DWARF 1 (*GID1*) gene (*BraA05g040050.3C*) [42], which was upregulated in MB and its log<sub>2</sub> ratio (MB\_GA/MB) was −1.142. In the GA biosynthetic process, *GA20ox2* (*BraA02g015640.3C*), *GA2ox2* (*BraA09g034980.3C*, *BraA08g023600.3C*), *GA2ox8* (*BraA01g011970.3C* and *BraA03g049490.3C*), and *GA3ox1* (*BraA09g058660.3C*) were upregulated in the MB\_GA. In the cellular response to GA stimulus process, *BraA06g028670.3C*, *BraA09g062830.3C*, and *BraA06g005530.3C* (bZIP transcription factor family protein) were upregulated and *BraA03g042690.3C* (gibberellin-regulated family protein) was downregulated. In response to GA<sub>3</sub> treatment, the *GASA10* gene (*BraA03g011100.3C*) was upregulated and the *GASA14* gene (*BraA03g006560.3C*) was downregulated (Figure 6B).

In the BR signal transduction pathway, two were upregulated (*BraA01g002030.3C* and *BraA02g030240.3C*), and two were downregulated (*BraA03g045210.3C* and *BraA02g022600.3C*) in MB\_GA. Four genes associated with ethylene metabolism were upregulated, including *BraA09g064090.3C*, *BraA01g030800.3C*, *BraA09g005890.3C*, and *BraA03g042600.3C* in MB\_GA compared to MB. Three JA-related genes, including *BraA02g020000.3C*, *BraA09g022310.3C*, and *BraA07g035430.3C*, were upregulated in MB\_GA compared to MB (Figure 6B).

### 3.5. qRT-PCR Analysis on DEGs Related to Auxin

To further confirm the accuracy of the RNA-seq data, 11 DEG-related auxin biosynthesis pathway genes that showed log<sub>2</sub> ratio  $\geq 2$  in expression between MB and MB\_GA were selected for qRT-PCR. These genes were *AUX1* (*BraA04g027030.3C*), *IAA29* (*BraA03g057220.3C*), *IAA1* (*BraA06g001750.3C*), *SAUR10* (*BraA09g053610.3C*), *SAUR21* (*BraA02g007500.3C*), *SAUR1* (*BraA01g003530.3C*), *SAUR59* (*BraA09g050440.3C*), *SAUR45* (*BraA05g009190.3C*), *SAUR16* (*BraA06g044670.3C*), *SAUR37* (*BraA04g000440.3C*), and *CH3.5* (*BraA03g053600.3C*) (Table S10). Correlation analysis showed that the high expression patterns of these genes that were selected by RNA-seq were consistent with the qRT-PCR data (Figure 7), thus indicating the dependability of the transcriptome results obtained in this study.

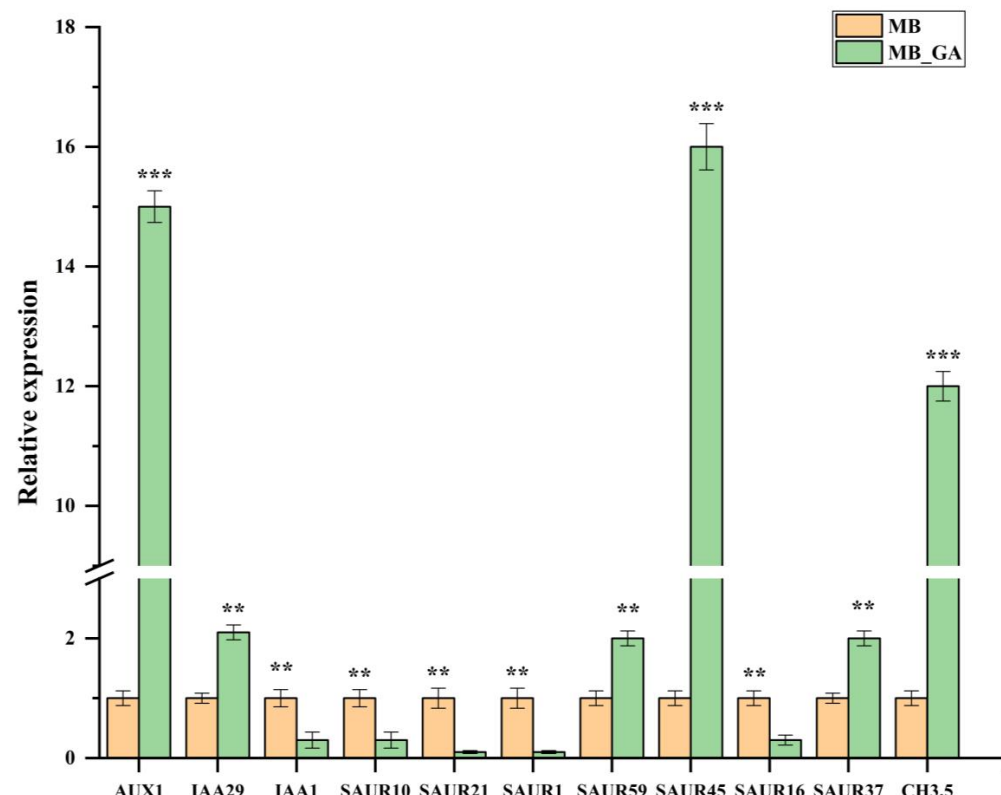


**Figure 7.** Expression profiles of 11 key differentially expressed genes (DEGs) in the MB and MB\_GA. Error bars represent the standard error of the mean for three biological replicates. \*\*  $p < 0.01$  and \*\*\*  $p < 0.001$  determined by Student's *t*-test.

### 3.6. Exogenous GA<sub>3</sub> Altered Auxin Contents in the Rosette Shoot

The content of auxin hormones was determined in the rosette shoot of MB and MB\_GA by HPLC (Figure 8). The auxin content significantly increased after spraying with GA<sub>3</sub>. The results indicated that auxin may contribute to the development of rosette branch numbers.

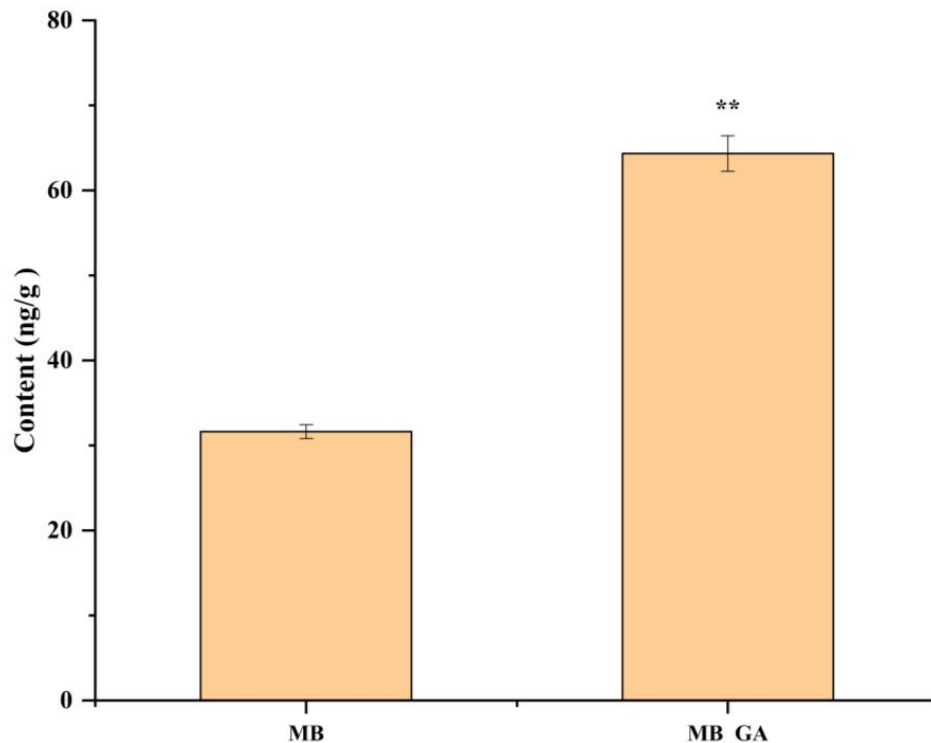


**Figure 8.** Determination of the content of auxin in MB and MB\_GA. \*\*  $p < 0.01$  determined by Student's *t*-test.

### 4. Discussion

The branching of the rosette shoot is crucial for increasing the yield of flowering Chinese cabbage. Previous studies have shown that the application of GA<sub>3</sub> reduced tillering in rice [43]. The overexpression of genes controlling GA<sub>3</sub> leads to reduced GA<sub>1</sub> levels producing increased branching phenotypes in pea [44], and treatment with higher concentrations of GA<sub>3</sub> inhibited the promotion of axillary bud (AB) outgrowth in apple trees [5]. Herein, we aimed to decipher the potential mechanism of exogenous GA<sub>3</sub> application to reduce the primary rosette branching in flowering Chinese cabbage. To this end, we firstly screened out a concentration of 600 mg/L GA<sub>3</sub> for spraying and found an increase in the length of the rosette shoots and a decrease in the primary rosette branching numbers. Following comparative transcriptome analysis and multiple phytohormone profiling by targeted metabolism, auxin has been found to be negatively regulated in rosette branching for flowering Chinese cabbage.

In this study, we detected 2183 genes that were differentially expressed between the multiple-branched Chinese flowering cabbage and GA treatment by RNA-seq, of which 1318 genes were upregulated and 865 genes were downregulated. The plant hormone signal transduction pathways were also significantly enriched by analyzing the functional annotation of the DEGs. The IAA signaling pathway had the highest number of DEGs, and transcriptome data indicated that the key genes in the IAA signaling pathway are all changing. Therefore, the genes involved in the IAA signaling pathway are of particular concern.

The degradation of Aux/IAA promoted by auxin is achieved by inhibiting the transcription of ARFs, and the degradation of Aux/IAA requires the participation of TIR1 [45–47].

The stability of the interaction between *Aux/IAA* and *TIR1* is mainly mediated by the binding of auxin to the F-box of *TIR1* [48–50]. The *TIR1/AFB Aux/IAA* pathway enhances the regulatory effect of *SAUR19*, and *SAUR19* is a very small family protein member that can be rapidly induced by auxin [51]. *Aux/IAAs* are believed to act as auxin-responsive proteins that mediate IAA signaling in the regulation of plant development [52]. Numerous studies have shown that *Aux/IAA* plays a significant role in regulating lateral branch development. The downregulation of *SIIAA2*, *SIIAA4*, *SIIAA7*, and *SIIAA9* has been found in transgenic tomatoes with multiple branches [53]. Furthermore, GA can also synergistically regulate axillary bud formation with IAA. The main influx and efflux of auxin rely on the polarity transport streams mediated by PIN and *Aux/IAA* proteins [54]. GA regulates *PIN* synthesis and accounts for auxin transport-dependent growth by the DELLA protein, which is a suppressor of GA biosynthesis and signal transduction [55]. It can also bind to the transcription factor SQUAMOSA PROMOTER BINDING PROTEIN-LIKE9 (SPL9) to facilitate axillary bud formation and regulate branching in *Arabidopsis* [19,56,57]. We identified DEGs of *AUX1*, *IAA29*, *SAUR1*, *SAUR10*, *SAUR16*, and *SAUR21* related to IAA metabolism and signal transduction between MB and MB\_GA, which suggested that auxin may be involved in the formation of rosette branches in flowering Chinese cabbage. IAA concentration was increased and the IAA-related genes *IAA2*, *IAA11*, and *IAA29* were highly expressed in response to GA treatment to inhibit branching [58]. Similar to the above research result, the content of auxin determined by HPLC has a significant increase in MB\_GA compared to MB. These results indicate that auxin may play an important role in flowering Chinese cabbage rosette branches.

Based on the results, we predicted a potential genetic mechanism of exogenous GA<sub>3</sub> application to reduce the primary rosette branching in flowering Chinese cabbage (Figure 9). It was speculated that exogenously sprayed GA<sub>3</sub> might upregulate the expression of *AUX1* influx carriers in specific areas of the rosette shoot, whereafter the *AUX1* might further induce the upregulated expression of the auxin receptor *TIR1*. *TIR1* and *AFB2* were shown to interact with *IAA29* by reducing the *IAA29* expression. The *TIR1/AFB-Aux/IAA-ARF* complex could directly or indirectly inhibit flowering Chinese cabbage rosette branches by suppressing the expression of *SAUR1*, *SAUR10*, *SAUR16*, and *SAUR21*.

The analysis of the hormone-responsive gene promoter region revealed various cis-regulatory elements like GA-responsive elements (GARE-motif, P-box) [59], auxin (TGA-element, AuxRR-core element and TATC-box) [60], ABA (ABRE element), ET (ERE element) [61], JA (MYC element, TGACG-motif) [62], SA (TCA-element) [63], etc., suggesting that they may have been involved in growth, development, and stress responses [64,65]. ARF24 combined with an auxin response region (AuxRR) affects kernel size in different maize haplotypes [66]. Two GARE-motif cis-acting elements are sufficient for gibberellin-upregulated proteinase expression in rice seeds [67]. In addition, the promoter of the gene in Figure 9 was analyzed (Table S11). The phytohormone-responsive cis-regulatory elements not only include GA-responsive elements (GARE-motif, P-box), but also many other hormone-responsive elements, including auxin (TGA-element, AuxRR-core element and TATC-box), ABA (ABRE element), JA (MYC element, TGACG-motif), SA (TCA-element), and ET (ERE element). This result indicates that auxin-related genes may respond to GA and various plant hormones to regulate branching development. Our results will be useful for elucidating the regulatory mechanisms of branching architecture in flowering Chinese cabbage.

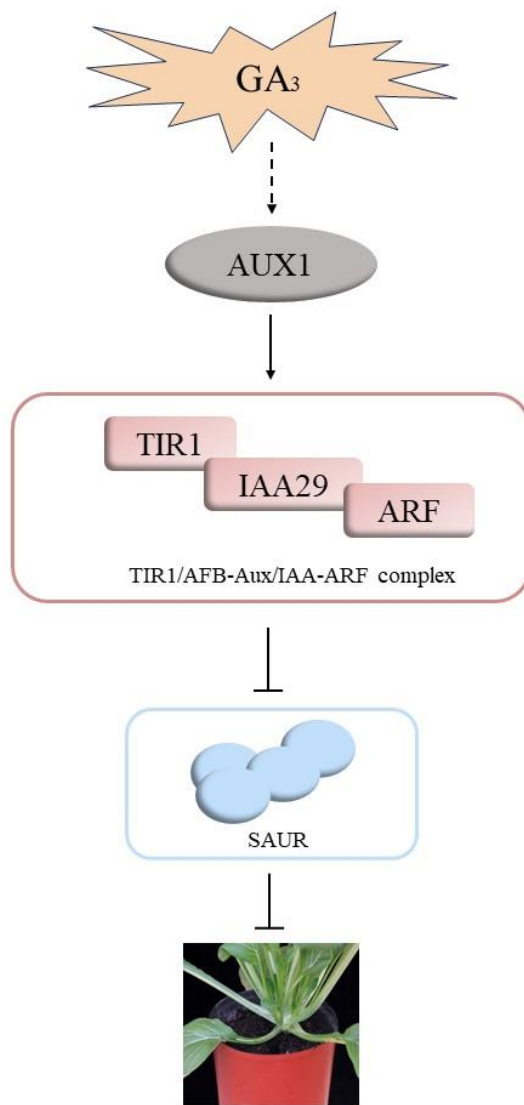


**Figure 9.** A hypothetical regulatory network of the rosette branching inhibited by exogenous  $\text{GA}_3$  in flowering Chinese cabbage.

## 5. Conclusions

According to the comprehensive experimental results,  $\text{GA}_3$  spraying can significantly decrease primary rosette branching in flowering Chinese cabbage, as well as influence the total and single plant yield. The transcriptome data indicate that  $\text{GA}_3$  can interact with auxin-related genes to reduce the number of branches on the rosette stems in flowering Chinese cabbage. Using metabolic profiling, we identified that the content of auxin was significantly increased in MB\_GA, which was highly associated with RNA-seq. Based on the above results, our results provide a new molecular mechanism for flowering Chinese cabbage branching, and can provide theoretical and practical guidance for its production.

**Supplementary Materials:** The following supporting information can be downloaded at: <https://www.mdpi.com/article/10.3390/agronomy14040762/s1>, Table S1. Summary of all expressed genes detected in the MB and MB\_GA libraries; Table S2. Summary of clean data detected in the MB and MB\_GA libraries; Table S3. Summary of GC content detected in the MB and MB\_GA libraries; Table S4. List of all genes detected in the MB and MB\_GA; Table S5. List of DEGs detected in the MB and MB\_GA; Table S6. Significantly enriched GO terms identified in the MB compared with MB\_GA; Table S7. Significantly enriched KEGG metabolic pathways in the MB compared with MB\_GA; Table S8. DEGs involved in the plant hormone; Table S9. Transcription factors identified

in the MB compared with MB\_GA; Table S10. Primer sequences used for the qRT-PCR analysis; Table S11. Table S11 Cis-acting elements in auxin related genes.

**Author Contributions:** Experiment, Data curation, Figures, Writing—original draft, X.Q.; Funding acquisition, Writing—review, Y.Z. (Ying Zhao); Literature search, Data investigation, N.C.; Experimental design, Data collection, J.G.; Software, Data visualization, Z.L. (Zeji Liu); Methodology, Data analysis, Z.L. (Zhiyong Liu); Writing—review and editing, H.F.; Experimental design, Conceptualization, Funding acquisition, Writing—review and editing, Y.Z. (Yun Zhang). All authors have read and agreed to the published version of the manuscript.

**Funding:** This work was financially supported by Science and Technology Project of Liaoning-Applied Basic Research Plan (Youth Special Project), No.2023JH2/101600054 and National Training Program of Innovation and Entrepreneurship for Undergraduate (202310163039).

**Data Availability Statement:** The RNA-Seq data of all samples have been submitted to GenBank of the National Center for Biotechnology Information (<https://www.ncbi.nlm.nih.gov/>), and the Sequence Read Archive (SRA) accession number is PRJNA777406.

**Conflicts of Interest:** The authors declare no conflicts of interest.

## References

- Lin, L.Z.; Harnly, J.M. Phenolic component profiles of mustard greens, yu choy, and 15 other brassica vegetables. *J. Agric. Food Chem.* **2010**, *58*, 6850–6857. [[CrossRef](#)] [[PubMed](#)]
- Teichmann, T.; Muhr, M. Shaping plant architecture. *Front. Plant Sci.* **2015**, *6*, 233. [[CrossRef](#)] [[PubMed](#)]
- Wang, M.; Moigne, M.L.; Bertheloot, J.; Crespel, L.; Perez-Garcia, M.D.; Ogé, L.; Demotes-Mainard, S.; Hamama, L.; Davière, J.M.; Sakr, S. BRANCHED1: A Key Hub of Shoot Branching. *Front. Plant Sci.* **2019**, *10*, 76. [[CrossRef](#)] [[PubMed](#)]
- Yang, Y.; Nicolas, M.; Zhang, J.; Yu, H.; Guo, D.; Yuan, R.; Zhang, T.; Yang, J.; Cubas, P.; Qin, G. The TIE1 transcriptional repressor controls shoot branching by directly repressing BRANCHED1 in Arabidopsis. *PLoS Genet.* **2018**, *14*, e1007296. [[CrossRef](#)] [[PubMed](#)]
- Jung, H.; Lee, D.K.; Choi, Y.D.; Kim, J.K. OsIAA6, a member of the rice Aux/IAA gene family, is involved in drought tolerance and tiller outgrowth. *Plant Sci.* **2015**, *236*, 304–312. [[CrossRef](#)] [[PubMed](#)]
- Bainbridge, K.; Guyomarc'h, S.; Bayer, E.; Swarup, R.; Bennett, M.; Mandel, T.; Kuhlemeier, C. Auxin influx carriers stabilize phyllotactic patterning. *Genes Dev.* **2008**, *22*, 810–823. [[CrossRef](#)] [[PubMed](#)]
- Liu, Y.; Xu, J.; Ding, Y.; Wang, Q.; Li, G.; Wang, S. Auxin inhibits the outgrowth of tiller buds in rice (*Oryza sativa* L.) by downregulating OsIPT expression and cytokinin biosynthesis in nodes. *Am. J. Crop Sci.* **2011**, *5*, 169–174.
- Reinhardt, D.; Pesce, E.R.; Stieger, P.; Mandel, T.; Baltensperger, K.; Bennett, M.; Traas, J.; Friml, J.; Kuhlemeier, C. Regulation of phyllotaxis by polar auxin transport. *Nature* **2003**, *426*, 255–260. [[CrossRef](#)]
- Vernoux, T.; Besnard, F.; Traas, J. Auxin at the shoot apical meristem. *Cold Spring Harb. Perspect. Biol.* **2010**, *2*, a001487. [[CrossRef](#)]
- Barbier, F.F.; Dun, E.A.; Kerr, S.C.; Chabikwa, T.G.; Beveridge, C.A. An Update on the Signals Controlling Shoot Branching. *Trends Plant Sci.* **2019**, *24*, 220–236. [[CrossRef](#)]
- Dierck, R.; Keyser, E.D.; Riek, J.D.; Dhooghe, E.; Huylenbroeck, J.V.; Prinsen, E.; Straeten, D.V.D. Change in Auxin and Cytokinin Levels Coincides with Altered Expression of Branching Genes during Axillary Bud Outgrowth in Chrysanthemum. *PLoS ONE* **2016**, *11*, e0161732. [[CrossRef](#)] [[PubMed](#)]
- Lin, Q.B.; Zhang, Z.; Wu, F.Q.; Feng, M.; Sun, Y.; Chen, W.W.; Cheng, Z.J.; Zhang, X.; Ren, Y.L.; Lei, C.I.; et al. The APC/C<sup>TE</sup> E3 Ubiquitin Ligase Complex Mediates the Antagonistic Regulation of Root Growth and Tillering by ABA and GA. *Plant Cell* **2020**, *32*, 1973–1987. [[CrossRef](#)] [[PubMed](#)]
- Wang, Y.; Sun, S.; Zhu, W.; Jia, K.; Yang, H.; Wang, X. Strigolactone/MAX2-induced degradation of brassinosteroid transcriptional effector BES1 regulates shoot branching. *Dev. Cell* **2013**, *27*, 681–688. [[CrossRef](#)] [[PubMed](#)]
- Yamaguchi, S. Gibberellin metabolism and its regulation. *Annu. Rev. Plant Biol.* **2008**, *59*, 225–251. [[CrossRef](#)] [[PubMed](#)]
- Hedden, P.; Phillips, A.L. Gibberellin metabolism: New insights revealed by the genes. *Trends Plant Sci.* **2000**, *5*, 523–530. [[CrossRef](#)] [[PubMed](#)]
- Eiichi, T.; Naohiko, Y.; Yoshio, M. Effect of Gibberellic Acid on Dwarf and Normal Pea Plants. *Physiol. Plant.* **1967**, *20*, 291–298. [[CrossRef](#)]
- Tan, M.; Li, G.; Liu, X.; Cheng, F.; Ma, J.; Zhao, C.; Zhang, D.; Han, M. Exogenous application of GA3 inactively regulates axillary bud outgrowth by influencing of branching-inhibitors and bud-regulating hormones in apple (*Malus domestica* Borkh.). *Mol. Genet. Genomics* **2018**, *293*, 1547–1563. [[CrossRef](#)]
- Tian, Y.T.; Wang, J.N.; Guo, H.P.; Qu, K.; Xu, D.; Hou, L.L.; Li, J.H. Transcriptome Analysis of Active Axillary Buds from Narrow-crown and Broad-crown Poplars Provides Insight into the Phytohormone Regulatory Network for Branching Angle. *Plant Mol. Biol. Report.* **2021**, *39*, 595–606. [[CrossRef](#)]
- Zhang, Q.Q.; Wang, J.G.; Wang, L.Y.; Wang, J.F.; Wang, Q.; Yu, P.; Bai, M.Y.; Fan, M. Gibberellin repression of axillary bud formation in *Arabidopsis* by modulation of DELLA-SPL9 complex activity. *J. Integr. Plant Biol.* **2020**, *62*, 421–432. [[CrossRef](#)]

20. Lo, S.F.; Yang, S.Y.; Chen, K.T.; Hsing, Y.I.; Zeevaart, J.A.; Chen, L.J.; Yu, S.M. A novel class of gibberellin 2-oxidases control semidwarfism, tillering, and root development in rice. *Plant Cell* **2008**, *20*, 2603–2618. [[CrossRef](#)]
21. Liao, Z.; Yu, H.; Duan, J.; Yuan, K.; Yu, C.; Meng, X.; Kou, L.; Chen, M.; Jing, Y.; Liu, G.; et al. SLR1 inhibits MOC1 degradation to coordinate tiller number and plant height in rice. *Nat. Commun.* **2019**, *10*, 2738. [[CrossRef](#)]
22. Mauriat, M.; Sandberg, L.G.; Moritz, M. Proper gibberellin localization in vascular tissue is required to control auxin-dependent leaf development and bud outgrowth in hybrid aspen. *Plant J.* **2011**, *67*, 805–816. [[CrossRef](#)]
23. Agharkar, M.; Lomba, P.; Altpeter, F.; Zhang, H.; Kenworthy, K.L.T. Stable expression of AtGA2ox1 in a low-input turfgrass (*Paspalum notatum* Flugge) reduces bioactive gibberellin levels and improves turf quality under field conditions. *Plant Biotechnol. J.* **2007**, *5*, 791–801. [[CrossRef](#)]
24. Caruana, J.C.; Sittmann, J.W.; Wang, W.P.; Liu, Z.C. Suppressor of Runnerless encodes a DELLA protein that controls runner formation for asexual reproduction in strawberry. *Mol. Plant* **2018**, *11*, 230–233. [[CrossRef](#)]
25. O’Neill, D.P.; Ross, J.J. Auxin regulation of the gibberellin pathway in pea. *Plant Physiol.* **2000**, *130*, 1974–1982. [[CrossRef](#)]
26. Tenreira, T.; Lange, M.J.P.; Lange, T.; Bres, C.; Labadie, M.; Monfort, A.; Hernould, M.; Rothan, C.; Denoyes, B. A Specific Gibberellin 20-Oxidase Dictates the Flowering-Runnering Decision in Diploid Strawberry. *Plant Cell* **2017**, *29*, 2168–2182. [[CrossRef](#)]
27. Elfving, D.; Visser, D.; Henry, J. Gibberellins stimulate lateral branch development in young sweet cherry trees in the orchard. *Int. J. Fruit Sci.* **2011**, *11*, 41–54. [[CrossRef](#)]
28. Choubane, D.; Rabot, A.; Mortreau, E.; Legourrierec, J.; Péron, T.; Foucher, F.; Ahcène, Y.; Pelleschi-Trvier, S.; Leduc, N.; Hamama, L. Photocontrol of bud burst involves gibberellin biosynthesis in *Rosa* sp. *J. Plant Physiol.* **2012**, *169*, 1271–1280. [[CrossRef](#)]
29. Katyayini, N.U.; Rinne, P.L.H.; Tarkowská, D.; Strnad, M.; van der Schoot, C. Dual Role of Gibberellin in Perennial Shoot Branching: Inhibition and Activation. *Front. Plant Sci.* **2020**, *11*, 529247. [[CrossRef](#)] [[PubMed](#)]
30. Guan, J.; Li, J.; Yao, Q.; Liu, Z.; Feng, H.; Zhang, Y. Identification of two tandem genes associated with primary rosette branching in flowering Chinese cabbage. *Front. Plant Sci.* **2022**, *19*, 1083528. [[CrossRef](#)] [[PubMed](#)]
31. Gordon, S.P.; Tseng, E.; Salamov, A.; Zhang, J.; Meng, X.; Zhao, Z.; Wang, Z. Widespread Polycistronic Transcripts in Fungi Revealed by Single-Molecule mRNA Sequencing. *PLoS ONE* **2015**, *10*, e0132628. [[CrossRef](#)]
32. Mortazavi, A.; Williams, B.A.; McCue, K.; Schaeffer, L.; Wold, B. Mapping and quantifying mammalian transcriptomes by RNA-Seq. *Nat. Methods* **2008**, *5*, 621–628. [[CrossRef](#)]
33. Rosa, M.; Hilal, M.; González, J.A.; Prado, F.E. Low-temperature effect on enzyme activities involved in sucrose-starch partitioning in salt-stressed and salt-acclimated cotyledons of quinoa (*Chenopodium quinoa* Willd.) seedlings. *Plant Physiol. Biochem.* **2019**, *47*, 300–307. [[CrossRef](#)] [[PubMed](#)]
34. Livak, K.J.; Schmittgen, T.D. Analysis of relative gene expression data using real-time quantitative PCR. *Methods* **2002**, *25*, 402–408. [[CrossRef](#)] [[PubMed](#)]
35. Benjamini, Y.; Hochberg, Y. Controlling the False Discovery Rate: A Practical and Powerful Approach to Multiple Testing. *J. R. Stat. Soc. B* **1995**, *57*, 289–300. [[CrossRef](#)]
36. Benjamini, Y.; Yekutieli, D. The Control of the False Discovery Rate in Multiple Testing under Dependency. *Ann. Stat.* **2001**, *29*, 1165–1188. [[CrossRef](#)]
37. Abdi, H. Bonferroni and Šidák corrections for multiple comparisons. In *Encyclopedia of Measurement and Statistics*; Salkind, N., Ed.; CiteSeerX: Princeton, NJ, USA, 2007; pp. 103–107.
38. Yuan, C.; Xi, L.; Kou, Y.; Zhao, Y.; Zhao, L. Current perspectives on shoot branching regulation. *Front. Agric. Sci. Eng.* **2015**, *2*, 38–52. [[CrossRef](#)]
39. Lee, M.S.; An, J.H.; Cho, H.T. Biological and molecular functions of two EAR motifs of Arabidopsis IAA7. *J. Plant Biol.* **2016**, *59*, 24–32. [[CrossRef](#)]
40. Liu, Y.; Wang, Q.; Ding, Y.; Li, G.H.; Xu, J.X.; Wang, S.H. Effects of external ABA, GA<sub>3</sub> and NAA on the tiller bud outgrowth of rice is related to changes in endogenous hormones. *Plant Growth Regul.* **2011**, *65*, 247–254. [[CrossRef](#)]
41. Cui, D.; Neill, S.J.; Tang, Z.; Cai, W. Gibberellin-regulated XET is differentially induced by auxin in rice leaf sheath bases during gravitropic bending. *J. Exp. Bot.* **2005**, *56*, 1327–1334. [[CrossRef](#)]
42. Fukazawa, J.; Ito, T.; Kamiya, Y.; Yamaguchi, S.; Takahashi, Y. Binding of GID1 to DELLAAs promotes dissociation of GAF1 from DELLA in GA dependent manner. *Plant Signal. Behav.* **2015**, *10*, e1052923. [[CrossRef](#)] [[PubMed](#)]
43. Tang, S.; Li, L.; Zhou, Q.Y.; Liu, W.Z.; Zhang, H.X.; Chen, W.Z.; Ding, Y.F. Expression of wheat gibberellins 2-oxidase gene induced dwarf or semi-dwarf phenotype in rice. *Cereal Res. Commun.* **2019**, *47*, 239–249. [[CrossRef](#)]
44. Nadeau, C.D.; Ozga, J.A.; Kurepin, L.V.; Jin, A.; Pharis, R.P.; Reinecke, D.M. Tissue-Specific Regulation of Gibberellin Biosynthesis in Developing Pea Seeds. *Plant Physiol.* **2011**, *156*, 897–912. [[CrossRef](#)] [[PubMed](#)]
45. Worley, C.K.; Zenser, N.; Ramos, J.; Rouse, D.; Leyser, O.; Theologis, A.; Callis, J. Degradation of AUXIAA proteins is essential for normal auxin signalling. *Plant J.* **2000**, *21*, 553–562. [[CrossRef](#)] [[PubMed](#)]
46. Tiwari, S.B.; Wang, X.J.; Hagen, G.; Guilfoyle, T.J. AUXIAA proteins are active repressors, and their stability and activity are modulated by auxin. *Plant Cell* **2001**, *13*, 2809–2822. [[CrossRef](#)] [[PubMed](#)]
47. Dharmasiri, N.; Dharmasiri, S.; Estelle, M. The F-box protein TIR1 is an auxin receptor. *Nature* **2005**, *435*, 441–445. [[CrossRef](#)] [[PubMed](#)]

48. Gray, W.M.; Kepinski, S.; Rouse, D.; Leyser, O.; Estelle, M. Auxin regulates SCF(TIR1)-dependent degradation of AUX/IAA proteins. *Nature* **2001**, *414*, 271–276. [[CrossRef](#)] [[PubMed](#)]
49. Jain, M.; Nijhawan, A.; Arora, R.; Agarwal, P.; Ray, S.; Sharma, P.; Kapoor, S.; Tyagi, A.K.; Khurana, J.P. F-box proteins in rice. Genome-wide analysis, classification, temporal and spatial gene expression during panicle and seed development, and regulation by light and abiotic stress. *Plant Physiol.* **2007**, *143*, 1467–1483. [[CrossRef](#)]
50. Trenner, J.; Poeschl, Y.; Grau, J.; Gogol-Döring, A.; Quint, M.; Delker, C. Auxin-induced expression divergence between *Arabidopsis* species may originate within the TIR1/AFB-AUX/IAA-ARF module. *J. Exp. Bot.* **2017**, *68*, 539–552. [[CrossRef](#)]
51. Spatz, A.K.; Lee, S.H.; Wenger, J.P.; Gonzalez, N.; Itoh, H.; Inzé, D.; Peer, W.A.; Murphy, A.S.; Overvoorde, P.J.; Gray, W.M. The SAUR19 subfamily of SMALL AUXIN UP RNA genes promote cell expansion. *Plant J.* **2012**, *70*, 978–1068. [[CrossRef](#)]
52. Lee, M.S.; Choi, H.-S.; Cho, H.-T. Branching the auxin signaling: Multiple players and diverse interactions. *J. Plant Biol.* **2013**, *56*, 130–137. [[CrossRef](#)]
53. Pattison, R.J.; Catala, C. Evaluating auxin distribution in tomato (*Solanum lycopersicum*) through an analysis of the PIN and AUX/LAX gene families. *Plant J.* **2012**, *70*, 585–598. [[CrossRef](#)] [[PubMed](#)]
54. Vanneste, S.; Friml, J. Auxin: A trigger for change in plant development. *Cell* **2009**, *36*, 005–016. [[CrossRef](#)] [[PubMed](#)]
55. Salanenka, Y.; Verstraeten, I.; Lofke, C.; Tabata, K.; Naramoto, S.; Glanc, M.; Friml, J. Gibberellin DELLA signaling targets the retromer complex to redirect protein trafficking to the plasma membrane. *Proc. Natl. Acad. Sci. USA* **2018**, *115*, 3716–3721. [[CrossRef](#)] [[PubMed](#)]
56. Harrison, B.R.; Masson, P.H. ARL2, ARG1 and PIN3 define a gravity signal transduction pathway in root statocytes. *Plant J.* **2008**, *53*, 380–392. [[CrossRef](#)] [[PubMed](#)]
57. Gou, J.; Fu, C.; Liu, S.; Tang, C.; Debnath, S.; Flanagan, A.; Ge, Y.; Tang, Y.; Jiang, Q.; Larson, P.R.; et al. The miR156-SPL4 module predominantly regulates aerial axillary bud formation and controls shoot architecture. *New Phytol.* **2017**, *216*, 829–840. [[CrossRef](#)] [[PubMed](#)]
58. Jia, S.H.; Chang, S.; Wang, H.M.; Chu, Z.L.; Xi, C.; Liu, J.; Zhao, H.P.; Han, S.C.; Wang, Y.D. Transcriptomic analysis reveals the contribution of auxin on the differentially developed caryopses on primary and secondary branches in rice. *J. Plant Physiol.* **2021**, *256*, 153310. [[CrossRef](#)] [[PubMed](#)]
59. Yuan, G.; He, S.; Bian, S.; Han, X.; Liu, K.; Cong, P. Genome-wide identification and expression analysis of major latex protein (MLP) family genes in the apple (*Malus domestica* borkh.) genome. *Gene* **2020**, *733*, 144275. [[CrossRef](#)] [[PubMed](#)]
60. Chandler, J.W. Auxin response factors. *Plant Cell Environ.* **2016**, *39*, 1014–1028. [[CrossRef](#)]
61. Singh, K.B.; Foley, R.C.; Oñate-Sánchez, L. Transcription factors in plant defense and stress responses. *Curr. Opin. Plant Biol.* **2002**, *5*, 430–436. [[CrossRef](#)]
62. Boter, M.; Ruiz-Rivero, O.; Abdeen, A.; Prat, S. Conserved MYC transcription factors play a key role in jasmonate signaling both in tomato and *Arabidopsis*. *Genes* **2004**, *18*, 1577–1591. [[CrossRef](#)]
63. Wu, Q.; Bai, J.; Tao, X.; Mou, W.; Luo, Z.; Mao, L. Synergistic effect of abscisic acid and ethylene on color development in tomato (*Solanum lycopersicum* L.) fruit. *Sci. Hortic.* **2018**, *235*, 169–180. [[CrossRef](#)]
64. Yang, C.; Shi, G.; Li, Y.; Luo, M.; Wang, H.; Wang, J.; Yuan, L.; Wang, Y.; Li, Y. Genome-Wide Identification of SnRK1 Catalytic α Subunit and FLZ Proteins in *Glycyrrhiza inflata* Bat. Highlights Their Potential Roles in Licorice Growth and Abiotic Stress Responses. *Int. J. Mol. Sci.* **2023**, *24*, 121. [[CrossRef](#)]
65. Pan, W.; Zheng, P.; Zhang, C.; Wang, W.; Li, Y.; Fan, T. The effect of ABRE BINDING FACTOR 4-mediated FYVE1 on salt stress tolerance in *arabidopsis*. *Plant Sci.* **2020**, *296*, 110489. [[CrossRef](#)]
66. Gao, J.; Zhang, L.; Du, H.; Dong, Y.; Zhen, S.; Wang, C.; Wang, Q.; Yang, J.; Zhang, P.; Zheng, X.; et al. An ARF24-ZmArf2 module influences kernel size in different maize haplotypes. *J. Integr. Plant Biol.* **2023**, *65*, 1767–1781. [[CrossRef](#)]
67. Keita, S.; Daisuke, Y. Two cis-acting elements necessary and sufficient for gibberellin-upregulated proteinase expression in rice seeds. *Plant J.* **2003**, *34*, 635–645. [[CrossRef](#)]

**Disclaimer/Publisher’s Note:** The statements, opinions and data contained in all publications are solely those of the individual author(s) and contributor(s) and not of MDPI and/or the editor(s). MDPI and/or the editor(s) disclaim responsibility for any injury to people or property resulting from any ideas, methods, instructions or products referred to in the content.